Revisiting the high-scale validity of Type-II seesaw model with novel LHC signature

Nivedita Ghosh
Department Of Theoretical Physics
IACS, Kolkata

Presented In WHEPP 2019

December 9, 2019

Outline

Based on the work: **arXiv:1711.06062**
Dilip Kumar Ghosh, NG, Ipsita Saha, Avirup Shaw

Motivation

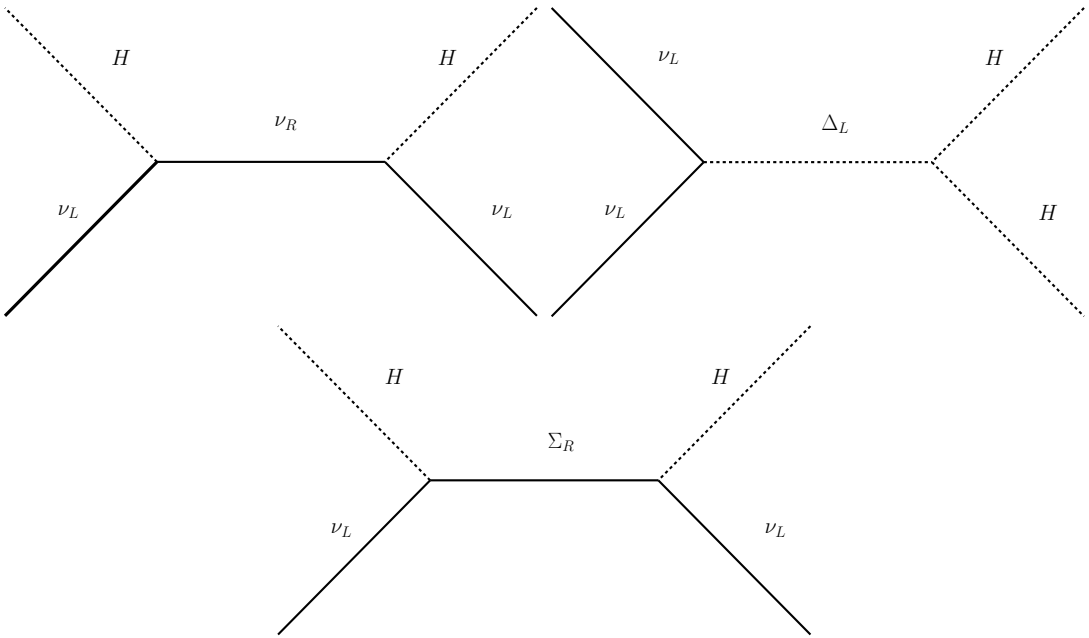

- Seek for absolute vacuum stability.

[1] J. Schechter et al,PhysRevD.22.2227

Motivation

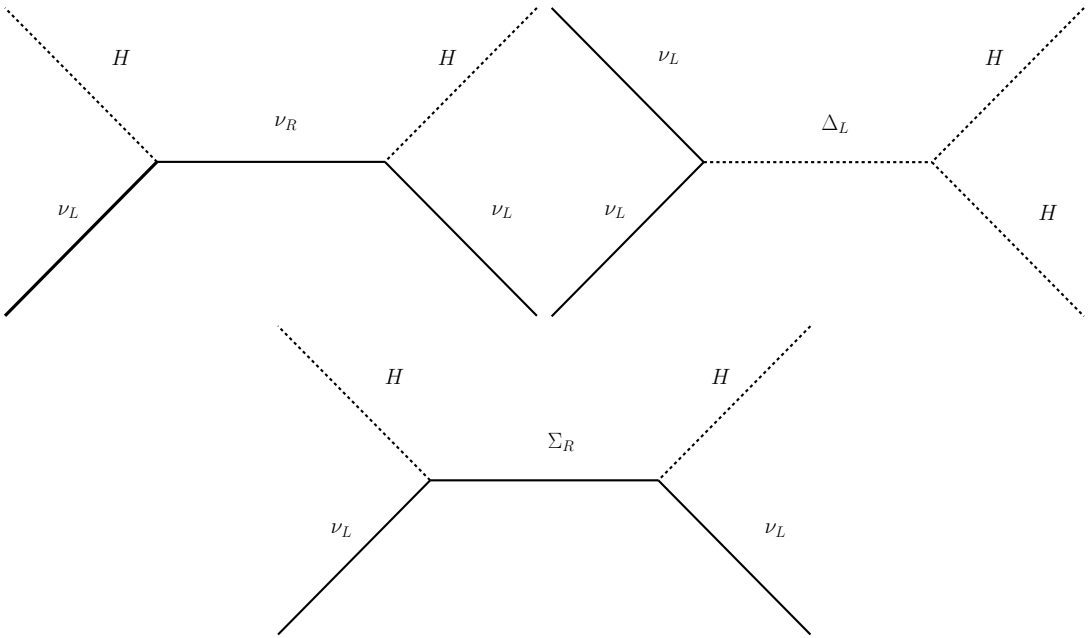

- Seek for absolute vacuum stability.
- Probe the Type-II seesaw model[1] parameter space allowed by all stability and perturbative unitary constraints.

[1] J. Schechter et al,PhysRevD.22.2227

Motivation

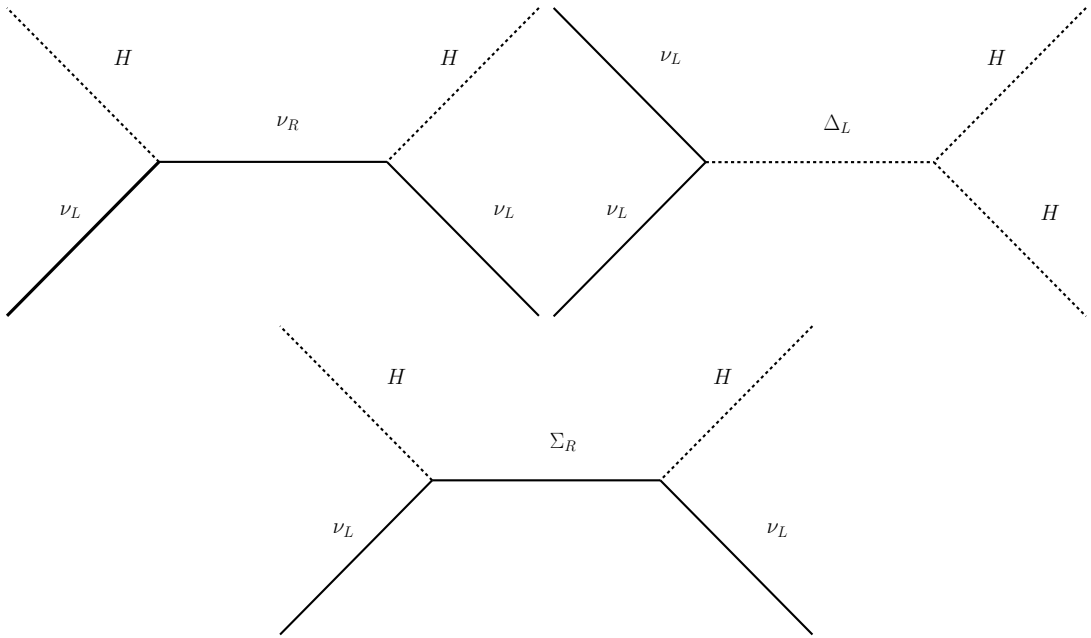

- Seek for absolute vacuum stability.
- Probe the Type-II seesaw model[1] parameter space allowed by all stability and perturbative unitary constraints.
- Examine the model prediction at the current and future run of the LHC.

[1] J. Schechter et al,PhysRevD.22.2227

Model

Type-II seesaw model contains an $SU(2)_L$ triplet scalar field Δ with hypercharge $Y = 2$ in addition to the SM fields.

$$\Delta \quad = \quad \frac{\sigma^i}{\sqrt{2}}\Delta_i = \begin{pmatrix} \delta^+/\sqrt{2} & \delta^{++} \\ \delta^0 & -\delta^+/\sqrt{2} \end{pmatrix}, \tag{1}$$

where $\Delta_1 = (\delta^{++} + \delta^0)/\sqrt{2},\ \Delta_2 = i(\delta^{++} - \delta^0)/\sqrt{2},\ \Delta_3 = \delta^+$.

Model

Type-II seesaw model contains an $SU(2)_L$ triplet scalar field Δ with hypercharge $Y = 2$ in addition to the SM fields.

$$\Delta = \frac{\sigma^i}{\sqrt{2}}\Delta_i = \begin{pmatrix} \delta^+/\sqrt{2} & \delta^{++} \\ \delta^0 & -\delta^+/\sqrt{2} \end{pmatrix}, \tag{1}$$

where $\Delta_1 = (\delta^{++} + \delta^0)/\sqrt{2},\ \Delta_2 = i(\delta^{++} - \delta^0)/\sqrt{2},\ \Delta_3 = \delta^+$.
The complete Lagrangian of this scenario is given by:

$$\mathcal{L} = \mathcal{L}_{\text{Yukawa}} + \mathcal{L}_{\text{Kinetic}} - V(\Phi, \Delta), \tag{2}$$

where the kinetic and Yukawa interactions are respectively.

$$\mathcal{L}_{\text{kinetic}} = (D_\mu \Phi)^\dagger (D^\mu \Phi) + \text{Tr}\left[(D_\mu \Delta)^\dagger (D^\mu \Delta)\right], \tag{3}$$

$$\mathcal{L}_{\text{Yukawa}} = \mathcal{L}^{\text{SM}}_{\text{Yukawa}} - (Y_\Delta)_{ij}\, L_i^{\mathsf{T}} C i\sigma_2 \Delta L_j + \text{h.c.} \tag{4}$$

Model

Type-II seesaw model contains an $SU(2)_L$ triplet scalar field Δ with hypercharge $Y = 2$ in addition to the SM fields.

$$\Delta \quad = \quad \frac{\sigma^i}{\sqrt{2}}\Delta_i = \begin{pmatrix} \delta^+/\sqrt{2} & \delta^{++} \\ \delta^0 & -\delta^+/\sqrt{2} \end{pmatrix}, \tag{1}$$

where $\Delta_1 = (\delta^{++} + \delta^0)/\sqrt{2},\ \Delta_2 = i(\delta^{++} - \delta^0)/\sqrt{2},\ \Delta_3 = \delta^+$.
The complete Lagrangian of this scenario is given by:

$$\mathcal{L} = \mathcal{L}_{\text{Yukawa}} + \mathcal{L}_{\text{Kinetic}} - V(\Phi, \Delta), \tag{2}$$

where the kinetic and Yukawa interactions are respectively.

$$\mathcal{L}_{\text{kinetic}} \quad = \quad (D_\mu \Phi)^\dagger (D^\mu \Phi) + \text{Tr}\left[(D_\mu \Delta)^\dagger (D^\mu \Delta)\right], \tag{3}$$

$$\mathcal{L}_{\text{Yukawa}} \quad = \quad \mathcal{L}^{\text{SM}}_{\text{Yukawa}} - (Y_\Delta)_{ij}\, L_i^{\mathsf{T}} C i\sigma_2 \Delta L_j + \text{h.c.} \tag{4}$$

Here $\Phi^{\mathsf{T}} = (\phi^+ \quad \phi^0)$ is the SM scalar doublet.

$$D_\mu \Delta = \partial_\mu \Delta + i\frac{g}{2}[\sigma^a W_\mu^a, \Delta] + ig' B_\mu \Delta \qquad (a = 1, 2, 3). \tag{5}$$

Model

The most general scalar potential[2] is given as :

$$V(\Phi,\Delta) = -m_\Phi^2(\Phi^\dagger\Phi) + \frac{\lambda}{4}(\Phi^\dagger\Phi)^2 + M_\Delta^2\,\mathrm{Tr}(\Delta^\dagger\Delta) + \left(\mu\Phi^\mathsf{T} i\sigma_2\Delta^\dagger\Phi + \mathrm{h.c.}\right) + \lambda_1(\Phi^\dagger\Phi)\mathrm{Tr}(\Delta^\dagger\Delta) + \lambda_2\left[\mathrm{Tr}(\Delta^\dagger\Delta)\right]^2 + \lambda_3\mathrm{Tr}(\Delta^\dagger\Delta)^2 + \lambda_4\Phi^\dagger\Delta\Delta^\dagger\Phi. \quad (6)$$

[2] A. Arhrib et al, PhysRevD.84.095005

Model

The most general scalar potential[2] is given as :

$$V(\Phi,\Delta) = -m_\Phi^2(\Phi^\dagger\Phi) + \frac{\lambda}{4}(\Phi^\dagger\Phi)^2 + M_\Delta^2\,\mathrm{Tr}(\Delta^\dagger\Delta) + \left(\mu\Phi^\mathsf{T} i\sigma_2\Delta^\dagger\Phi + \mathrm{h.c.}\right) + \lambda_1(\Phi^\dagger\Phi)\mathrm{Tr}(\Delta^\dagger\Delta) + \lambda_2\left[\mathrm{Tr}(\Delta^\dagger\Delta)\right]^2 + \lambda_3\mathrm{Tr}(\Delta^\dagger\Delta)^2 + \lambda_4\Phi^\dagger\Delta\Delta^\dagger\Phi. \quad (6)$$

After the EWSB, the minimization of the potential calculates the two mass parameters as,

$$m_\Phi^2 = \lambda\frac{v_d^2}{4} - \sqrt{2}\mu v_t + \frac{(\lambda_1+\lambda_4)}{2}v_t^2\,, \quad (7)$$

$$M_\Delta^2 = \frac{\mu v_d^2}{\sqrt{2}v_t} - \frac{\lambda_1+\lambda_4}{2}v_d^2 - (\lambda_2+\lambda_3)v_t^2\,, \quad (8)$$

The triplet vev (v_t) contributes to the electroweak gauge boson masses M_W^2 and M_Z^2 at tree level, $M_W^2 = \frac{g^2(v_d^2+2v_t^2)}{4}$ and $M_Z^2 = \frac{g^2(v_d^2+4v_t^2)}{4\cos^2\theta_W}$ respectively. The SM ρ-parameter is given by:

$$\rho = \frac{M_W^2}{M_Z^2\cos^2\theta_W} = \frac{1+\frac{2v_t^2}{v_d^2}}{1+\frac{4v_t^2}{v_d^2}}\,. \quad (9)$$

[2] A. Arhrib et al, PhysRevD.84.095005

model

One gets an upper bound on $\frac{v_t}{v_d} < 0.02$ or $v_t < 5$ GeV.

model

One gets an upper bound on $\frac{v_t}{v_d} < 0.02$ or $v_t < 5$ GeV.
After EWSB, the scalar fields expanded around respective vevs, can be parameterized as

$$\Phi = \frac{1}{\sqrt{2}} \begin{pmatrix} \sqrt{2}\chi_d^+ \\ v_d + h_d + i\eta_d \end{pmatrix} \qquad \Delta = \frac{1}{\sqrt{2}} \begin{pmatrix} \delta^+ & \sqrt{2}\delta^{++} \\ v_t + h_t + i\eta_t & -\delta^+ \end{pmatrix} \quad (10)$$

model

One gets an upper bound on $\frac{v_t}{v_d} < 0.02$ or $v_t < 5$ GeV.
After EWSB, the scalar fields expanded around respective vevs, can be parameterized as

$$\Phi = \frac{1}{\sqrt{2}} \begin{pmatrix} \sqrt{2}\chi_d^+ \\ v_d + h_d + i\eta_d \end{pmatrix} \qquad \Delta = \frac{1}{\sqrt{2}} \begin{pmatrix} \delta^+ & \sqrt{2}\delta^{++} \\ v_t + h_t + i\eta_t & -\delta^+ \end{pmatrix} \quad (10)$$

As a consequence, the scalar spectrum contains seven physical Higgs bosons: two doubly charged $H^{\pm\pm}$, two singly charged $H^{\pm}$, two CP-even neural (h, H) and a CP-odd (A) Higgs particles.

model

One gets an upper bound on $\frac{v_t}{v_d} < 0.02$ or $v_t < 5$ GeV.
After EWSB, the scalar fields expanded around respective vevs, can be parameterized as

$$\Phi = \frac{1}{\sqrt{2}} \begin{pmatrix} \sqrt{2}\chi_d^+ \\ v_d + h_d + i\eta_d \end{pmatrix} \qquad \Delta = \frac{1}{\sqrt{2}} \begin{pmatrix} \delta^+ & \sqrt{2}\delta^{++} \\ v_t + h_t + i\eta_t & -\delta^+ \end{pmatrix} \quad (10)$$

As a consequence, the scalar spectrum contains seven physical Higgs bosons: two doubly charged $H^{\pm\pm}$, two singly charged $H^{\pm}$, two CP-even neural (h, H) and a CP-odd (A) Higgs particles.
The corresponding mixing angles are given as

$$\tan\beta' = \frac{\sqrt{2}v_t}{v_d}, \quad \tan\beta = \frac{2v_t}{v_d} \equiv \sqrt{2}\tan\beta' \quad (11a)$$

$$\text{and} \quad \tan 2\alpha = \frac{2\mathcal{B}}{\mathcal{A} - \mathcal{C}}, \quad (11b)$$

$$\text{where,} \quad \mathcal{A} = \frac{\lambda}{2}v_d^2, \qquad \mathcal{B} = v_d[-\sqrt{2}\mu + (\lambda_1 + \lambda_4)v_t], \quad \mathcal{C} = \frac{\sqrt{2}\mu v_d^2 + 4(\lambda_2 + \lambda_3)v_t^3}{2v_t} \quad (11c)$$

model

$$\lambda = \frac{2}{v_d^2}(c_\alpha^2 m_h^2 + s_\alpha^2 m_H^2)\,, \tag{12a}$$

$$\lambda_1 = \frac{4m_{H^\pm}^2}{v_d^2+2v_t^2} - \frac{2m_A^2}{v_d^2+4v_t^2} + \frac{\sin 2\alpha}{2v_d v_t}(m_h^2 - m_H^2)\,, \tag{12b}$$

$$\lambda_2 = \frac{1}{v_t^2}\left[\frac{1}{2}\left(s_\alpha^2 m_h^2 + c_\alpha^2 m_H^2\right) + \frac{1}{2}\frac{v_d^2 m_A^2}{v_d^2+4v_t^2} - \frac{2v_d^2 m_{H^\pm}^2}{v_d^2+2v_t^2} + m_{H^{\pm\pm}}^2\right]\,, \tag{12c}$$

$$\lambda_3 = \frac{1}{v_t^2}\left[\frac{2v_d^2 m_{H^\pm}^2}{v_d^2+2v_t^2} - m_{H^{\pm\pm}}^2 - \frac{v_d^2 m_A^2}{v_d^2+4v_t^2}\right]\,, \tag{12d}$$

$$\lambda_4 = \frac{4m_A^2}{v_d^2+4v_t^2} - \frac{4m_{H^\pm}^2}{v_d^2+2v_t^2}\,, \tag{12e}$$

$$\mu = \frac{\sqrt{2}v_t m_A^2}{v_d^2+4v_t^2}\,. \tag{12f}$$

Vacuum stability

$$\lambda \geq 0\,, \tag{13a}$$
$$\lambda_2 + \lambda_3 \geq 0\,, \tag{13b}$$
$$\lambda_2 + \frac{\lambda_3}{2} \geq 0, \tag{13c}$$
$$\lambda_1 + \sqrt{\lambda(\lambda_2 + \lambda_3)} \geq 0\,, \tag{13d}$$
$$\lambda_1 + \sqrt{\lambda\left(\lambda_2 + \frac{\lambda_3}{2}\right)} \geq 0, \tag{13e}$$
$$\lambda_1 + \lambda_4 + \sqrt{\lambda(\lambda_2 + \lambda_3)} \geq 0\,, \tag{13f}$$
$$\lambda_1 + \lambda_4 + \sqrt{\lambda\left(\lambda_2 + \frac{\lambda_3}{2}\right)} \geq 0. \tag{13g}$$

Perturbative unitarity

$$
\begin{aligned}
|\lambda_1 + \lambda_4| &\leq 16\pi\,, \text{(14a)}\\
|\lambda_1| &\leq 16\pi\,, \text{(14b)}\\
|2\lambda_1 + 3\lambda_4| &\leq 32\pi\,, \text{(14c)}\\
|\lambda| &\leq 32\pi\,, \text{(14d)}\\
|\lambda_2| &\leq 8\pi\,, \quad \text{(14e)}\\
|\lambda_2 + \lambda_3| &\leq 8\pi\,, \quad \text{(14f)}\\
|\lambda + 4\lambda_2 + 8\lambda_3 \pm \sqrt{(\lambda - 4\lambda_2 - 8\lambda_3)^2 + 16\lambda_4^2}| &\leq 64\pi\,, \text{(14g)}\\
|3\lambda + 16\lambda_2 + 12\lambda_3 \pm \sqrt{(3\lambda - 16\lambda_2 - 12\lambda_3)^2 + 24(2\lambda_1 + \lambda_4)^2}| &\leq 64\pi\,, \text{(14h)}\\
|2\lambda_1 - \lambda_4| &\leq 16\pi\,, \quad \text{(14i)}\\
|2\lambda_2 - \lambda_3| &\leq 16\pi. \quad \text{(14j)}
\end{aligned}
$$

- **Constraints from electroweak precision test**: The strongest bound comes from the T-parameter which imposes strict limit on the mass splitting between the doubly and singly charged scalars, $\Delta M \equiv \mid m_{H^{\pm\pm}} - m_{H^{\pm}} \mid$ which should be $\lesssim 50$ GeV[3].

[3] E. J. Chun et al.,JHEP11(2012)106
[4] ATLAS collaboration

- **Constraints from electroweak precision test**: The strongest bound comes from the T-parameter which imposes strict limit on the mass splitting between the doubly and singly charged scalars, $\Delta M \equiv \mid m_{H^{\pm\pm}} - m_{H^{\pm}} \mid$ which should be $\lesssim 50$ GeV[3].
- **Experimental bounds on scalar masses** : The direct search on the singly charged scalar at the LEP II puts a limit on $m_{H^{\pm}} \geq 78$ GeV. For $v_t < 10^{-4}$ GeV (corresponds to large Yukawa couplings) and assuming degenerate scalars, the doubly charged Higgs boson decays to like sign dilepton (LSD) $\ell^{\pm}\ell^{\pm}$ with almost 100% probability. From the direct search of the doubly charged Higgs boson at 13 TeV LHC run, the current lower bound at 95% CL on its mass is $m_{H^{\pm\pm}} > 700 - 800$ GeV[4] depending upon the final state lepton flavor.

[3] E. J. Chun et al.,JHEP11(2012)106

[4] ATLAS collaboration

- **Constraints from electroweak precision test**: The strongest bound comes from the T-parameter which imposes strict limit on the mass splitting between the doubly and singly charged scalars, $\Delta M \equiv \mid m_{H^{\pm\pm}} - m_{H^{\pm}} \mid$ which should be $\lesssim 50$ GeV[3].
- **Experimental bounds on scalar masses** : The direct search on the singly charged scalar at the LEP II puts a limit on $m_{H^{\pm}} \geq 78$ GeV. For $v_t < 10^{-4}$ GeV (corresponds to large Yukawa couplings) and assuming degenerate scalars, the doubly charged Higgs boson decays to like sign dilepton (LSD) $\ell^{\pm}\ell^{\pm}$ with almost 100% probability. From the direct search of the doubly charged Higgs boson at 13 TeV LHC run, the current lower bound at 95% CL on its mass is $m_{H^{\pm\pm}} > 700 - 800$ GeV[4] depending upon the final state lepton flavor.
- **Constraints from Higgs signal strength**: Our choice of benchmark points remain within the 2σ limit of the current experimental bound ($0.85^{+0.22}_{-0.20}$) of the Higgs to diphoton signal strength.

[3] E. J. Chun et al.,JHEP11(2012)106

[4] ATLAS collaboration

High Scale Stability

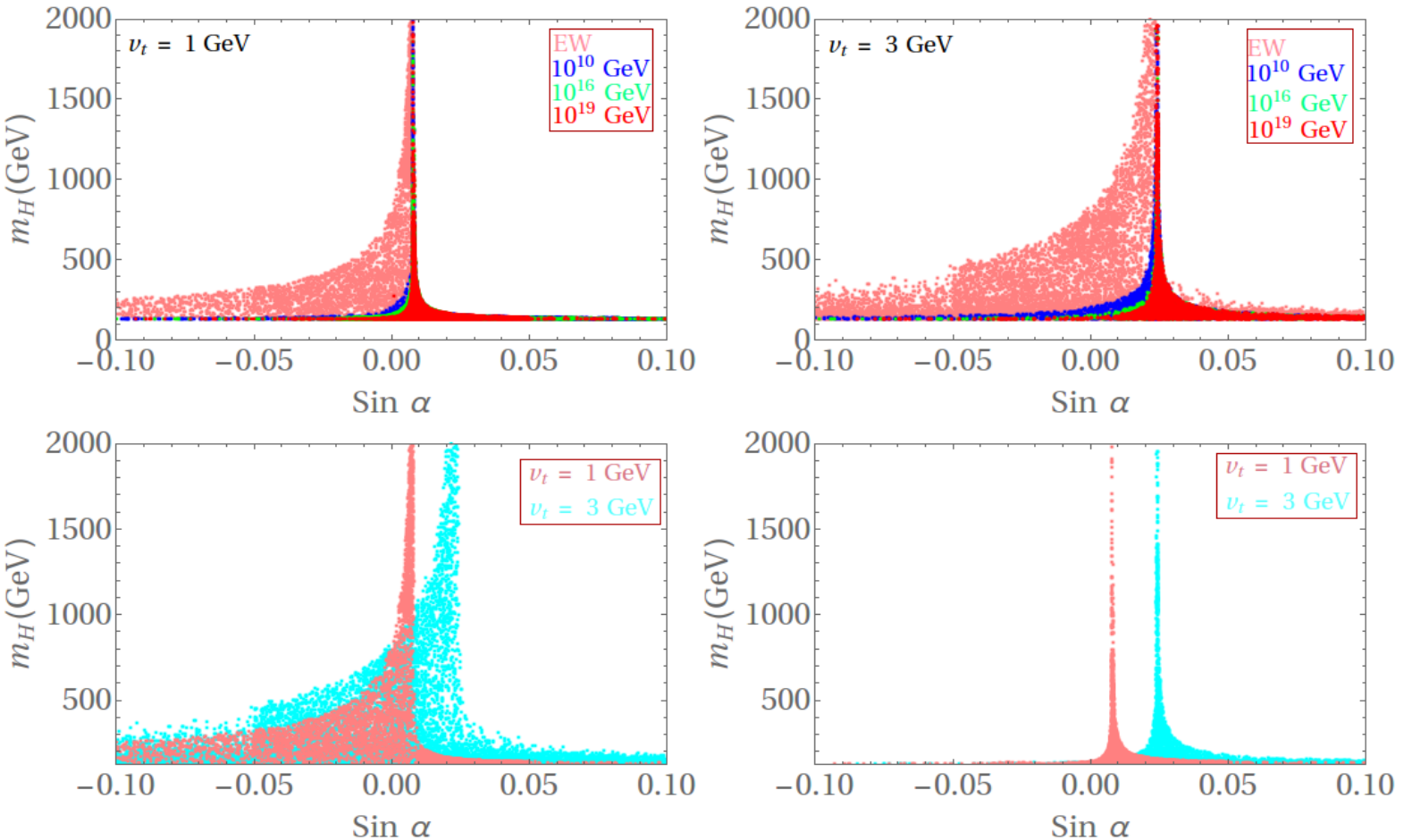

Figure: *(Upper panel) The valid parameter space in the* $\sin\alpha - m_H$ *plane for* $v_t = 1$ GeV *(left) and* $v_t = 3$ GeV *(right) for different values of cut-off scale.(Lower panel) The explicit distinction between the allowed parameter space by the two different* v_t *valid only at the EW scale(left) and all the way up to the Planck scale(right).*

High Scale stability

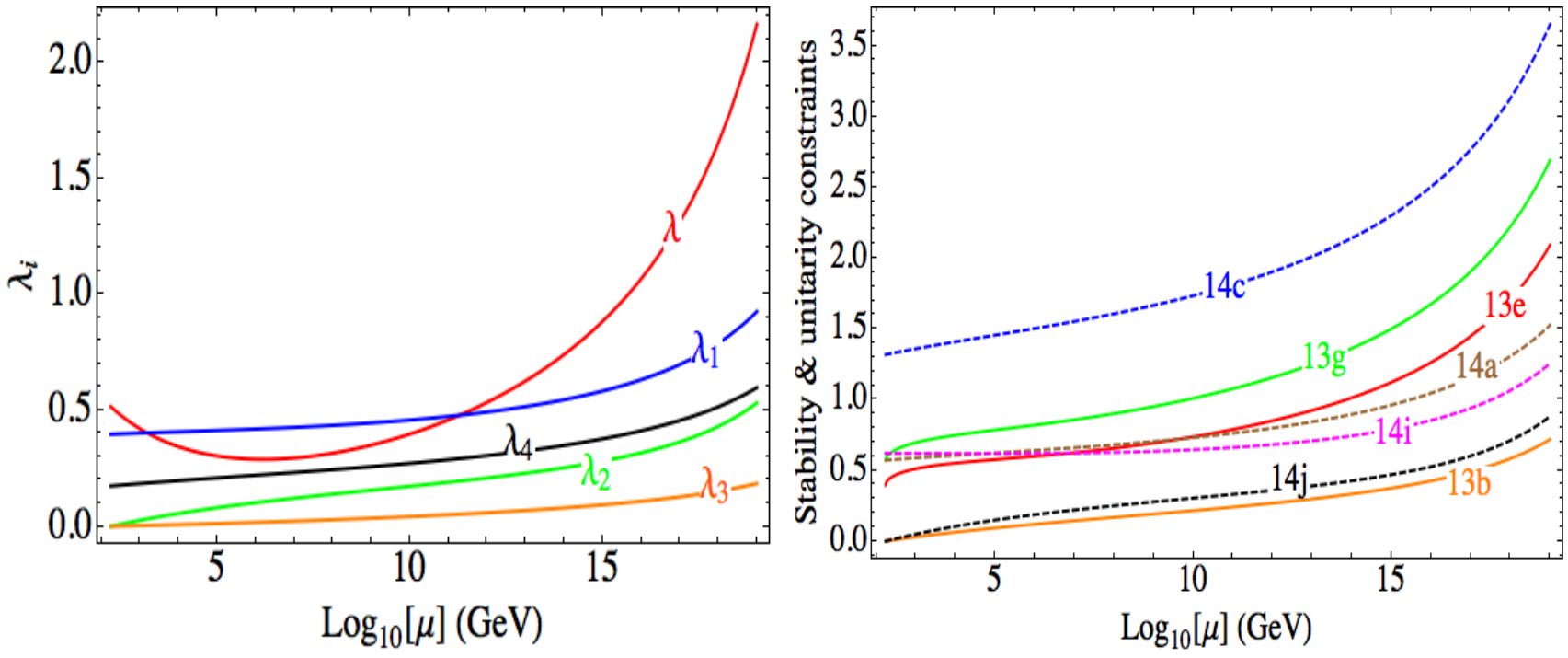

Figure: *(Left panel) The running of the five scalar quartic couplings up to the Planck scale for the benchmark point BP1 of positive scenario. (Right panel) The running of some of the stability and unitarity constraints indicated by the corresponding equation numbers for the same benchmark point.*

High Scale stability

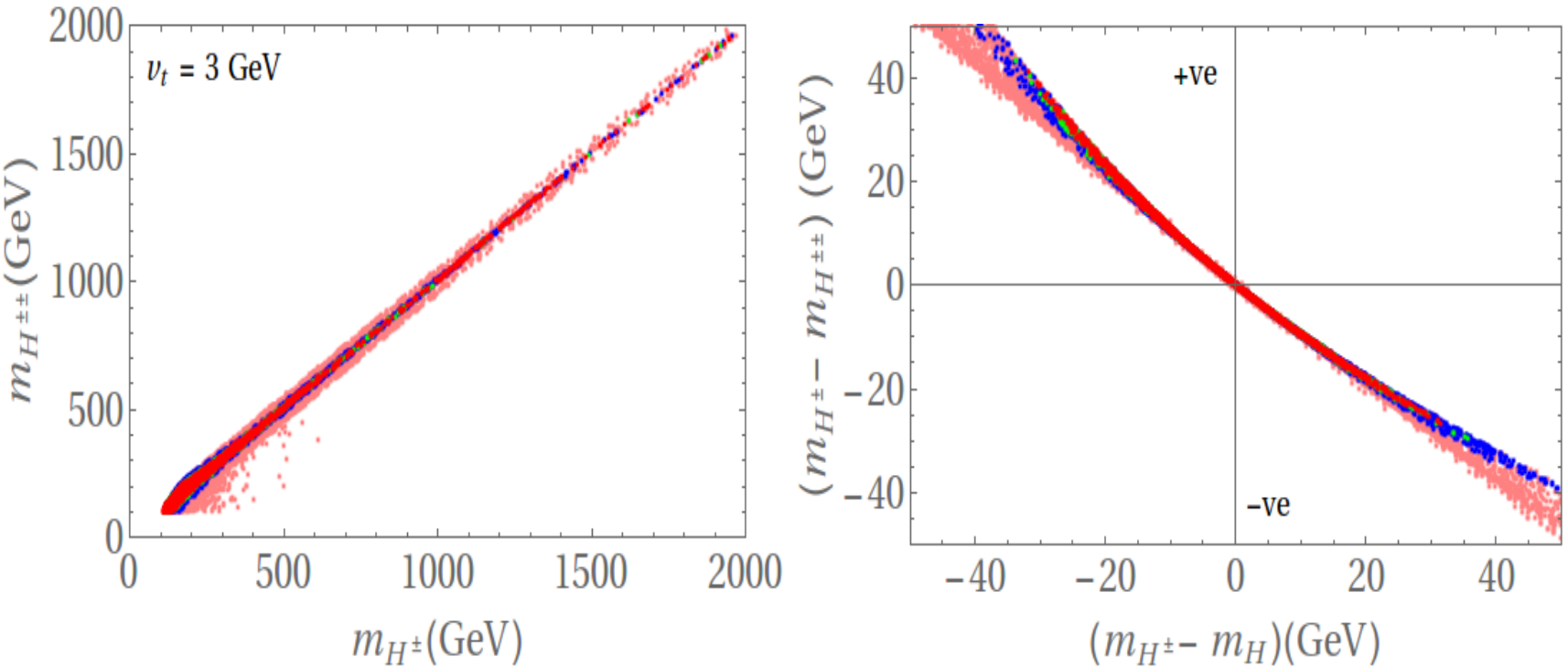

Figure: *(Left panel) The allowed parameter space in the $m_{H^\pm} - m_{H^{\pm\pm}}$ plane for triplet vev $v_t = 3$ GeV. The different colors follow the same convention as in Fig. 1. (Right panel) The corresponding allowed parameter space to show the relation between the mass splittings of the singly charged Higgs to the neutral Higgs $(m_{H^\pm} - m_H)$ and singly charged Higgs to the doubly charged Higgs $(m_{H^\pm} - m_{H^{\pm\pm}})$. The upper left square corresponds to the valid region for our positive scenario while the lower right corner denotes the same but for our negative scenario.*

Collider Analysis

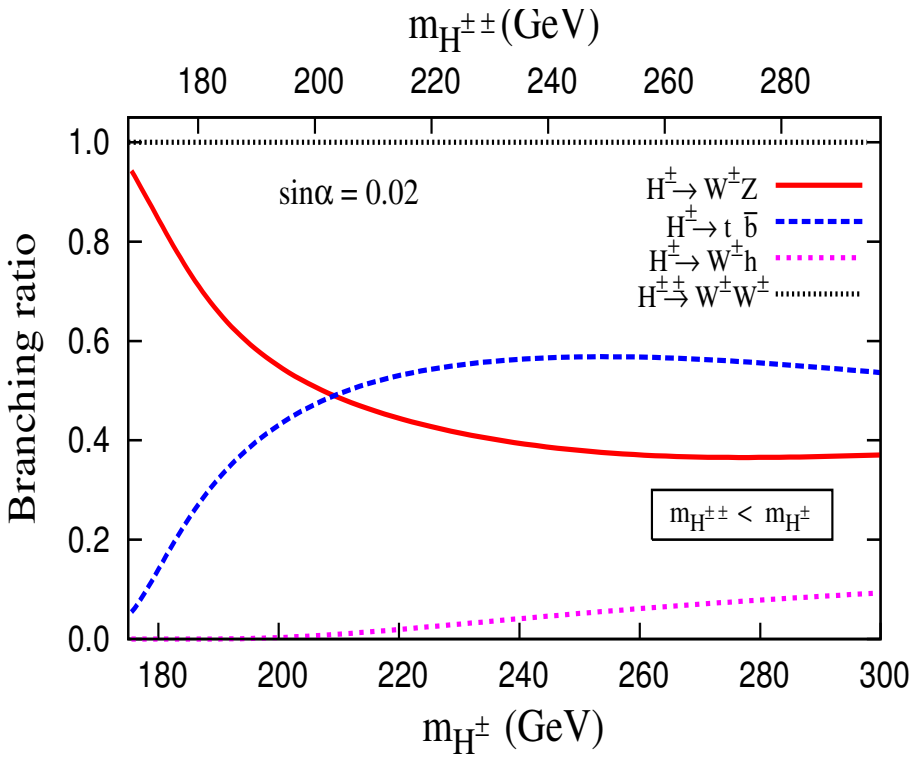

Figure: *Branching ratio of different two body decay modes for the doubly charged and singly charged scalars for* $\sin\alpha = 0.02$ *and* $v_t = 3$ GeV *for the positive scenario.*

Collider Analysis

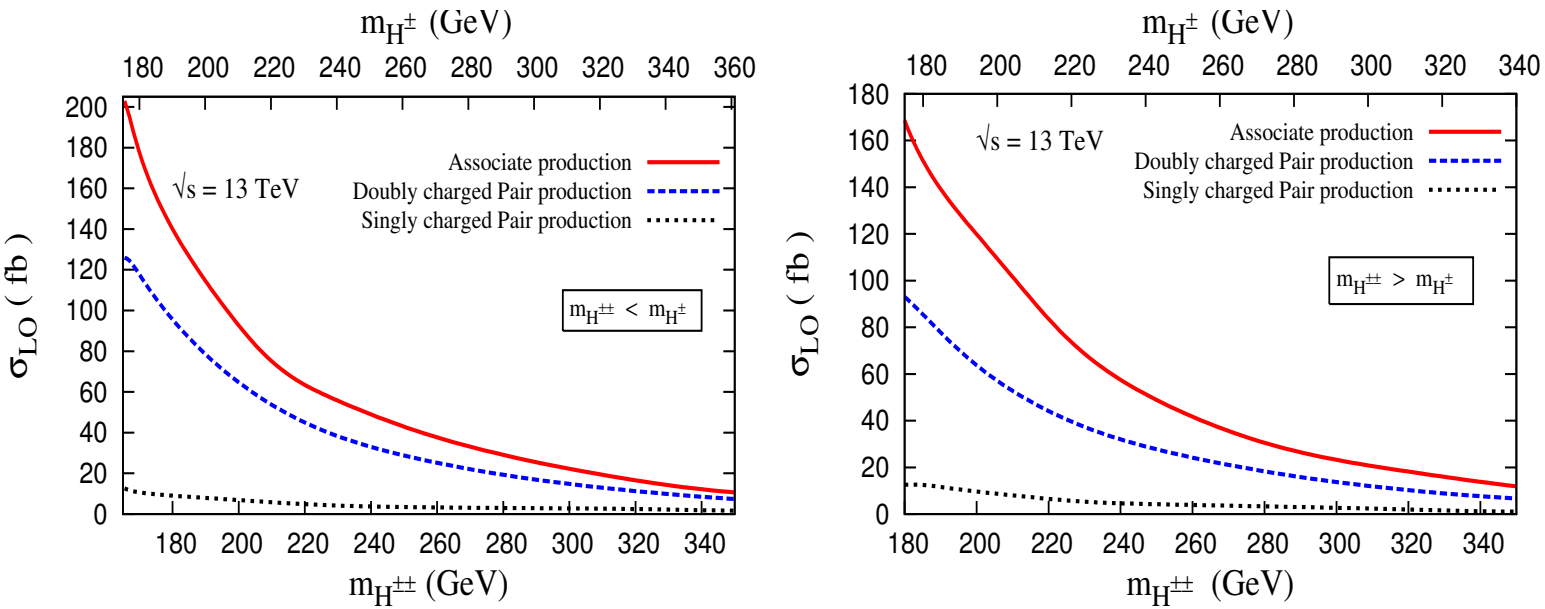

Figure: *Left (Right) panel shows the variation of* $\sigma_{\rm LO}(pp \to H^{\pm\pm}H^{\mp})$ (fb) *(solid red curve),* $\sigma_{\rm LO}(pp \to H^{++}H^{--})$ (fb) *(blue dashed curve) and* $\sigma_{\rm LO}(pp \to H^{+}H^{-})$ (fb) *(black dotted curve) with respect to charged Higgs masses at the LHC at* $\sqrt{s} = 13$ TeV *for positive (negative) scenario.*

Benchmark Points

Mass Scenario	$\sin\alpha$	$m_{H^{\pm\pm}}$ (GeV)	$m_{H^{\pm}}$ (GeV)	$m_H = m_A$ (GeV)	$\mu_{\gamma\gamma}$
Positive					
BP1	0.0220	165.48	173.25	180.70	0.79
BP2	0.0280	175.99	177.47	178.93	0.82
Negative					
BP1	0.0277	179.60	176.30	173.01	0.79
BP2	0.0300	184.17	180.11	175.95	0.81

Table: *Benchmark points valid by the high-scale stability constraints up to the Planck scale and their corresponding Higgs to diphoton signal strength ($\mu_{\gamma\gamma}$) for both the positive and the negative scenario.*

.

We consider the following two signal topologies:

$$(i) \quad 3\ell^{\pm} + \not{E}_T;$$
$$(ii) \quad (\ell^+\ell^+) + 4j + \not{E}_T,$$

Several SM processes contribute as backgrounds to the aforementioned two final states. We consider the following SM processes in our analysis: $t\bar{t}$+jets (up to 3), single top with three hard jets, V + jets (up to 3 jets), $V \equiv W^{\pm}, Z$, VV+ 3 jets, $t\bar{t} + (W^{\pm}/Z/h)$, and VVV.

$3\ell^{\pm} + \not{E}_T$

$$pp \to H^{++}H^{-} \to (W^{+}W^{+}) + (W^{-}Z) \to (\ell^{+}\ell^{+}) + \ell^{-} + \not{E}_T.$$

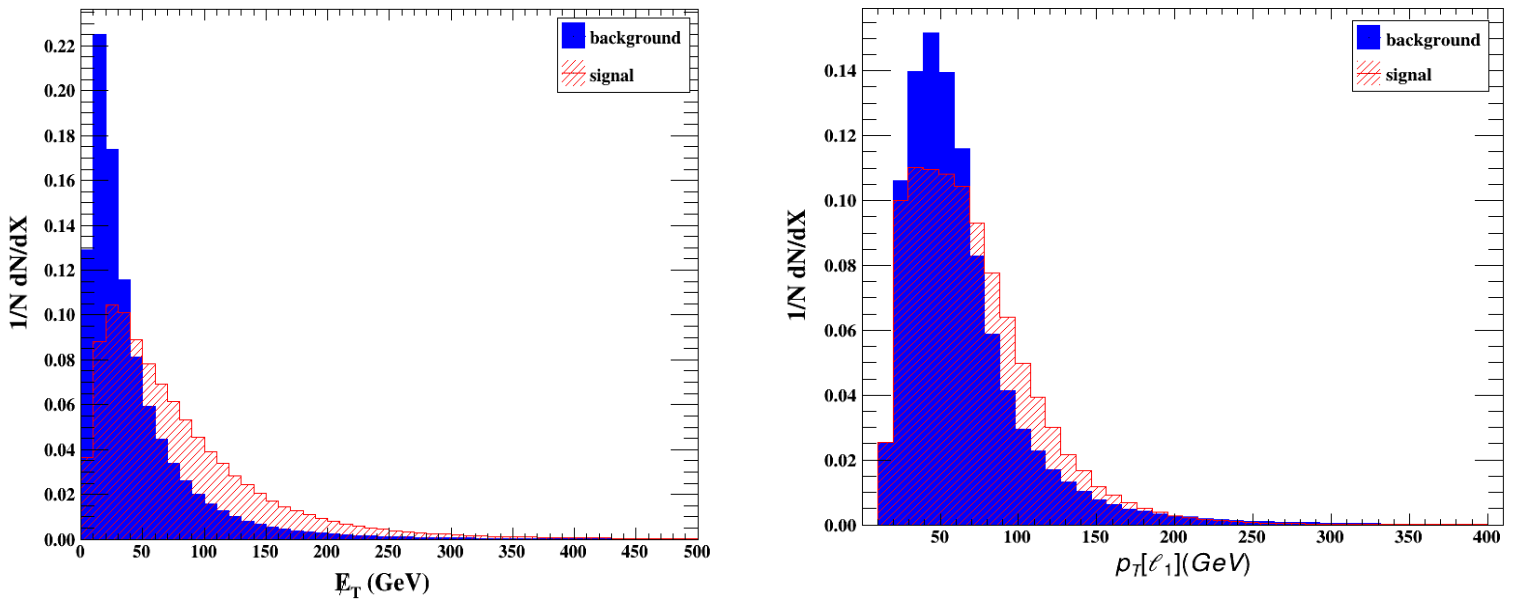

Figure: *Normalized distribution of the (left panel) Missing transverse energy ($\not{E}_T$) and (right panel) the transverse momentum of the hardest lepton ($p_T(\ell_1)$) after the basic kinematical acceptance cuts for the benchmark BP1 of positive scenario.*

$3\ell^{\pm} + \not{E}_T$

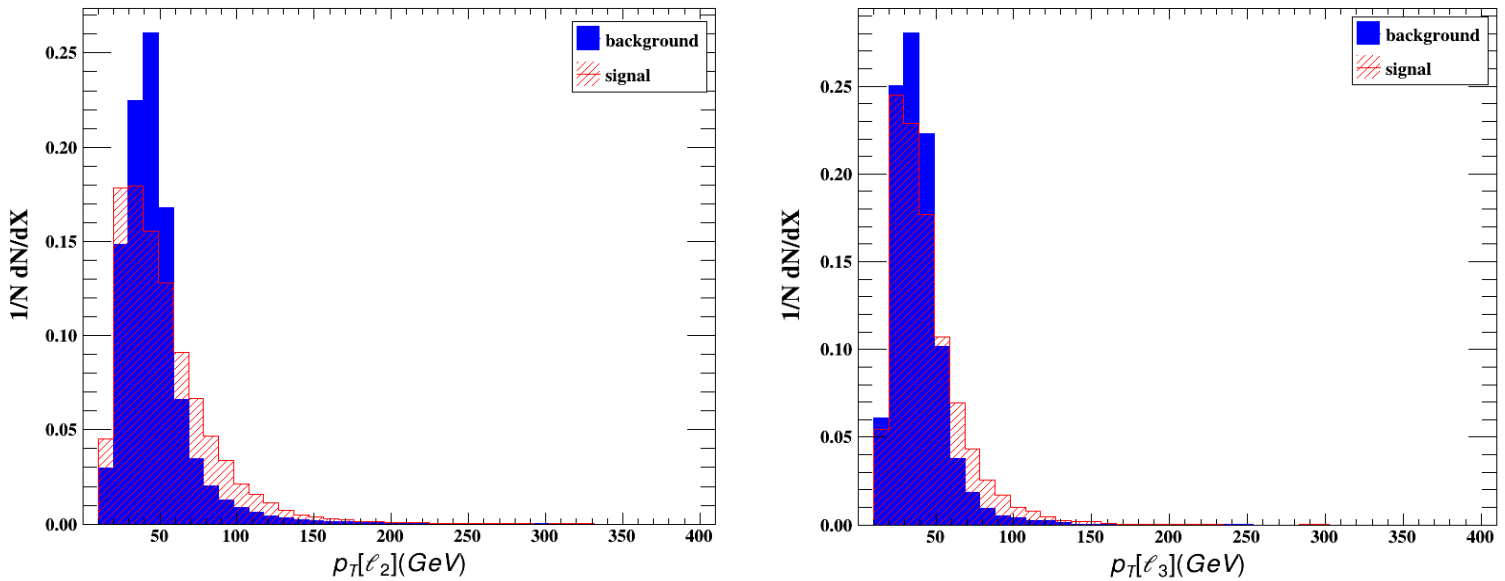

Figure: *Transverse momentum (p_T) distribution (normalized) of the two sub-leading leptons for the benchmark BP1 of positive scenario.*

$3\ell^{\pm} + \not{E}_T$

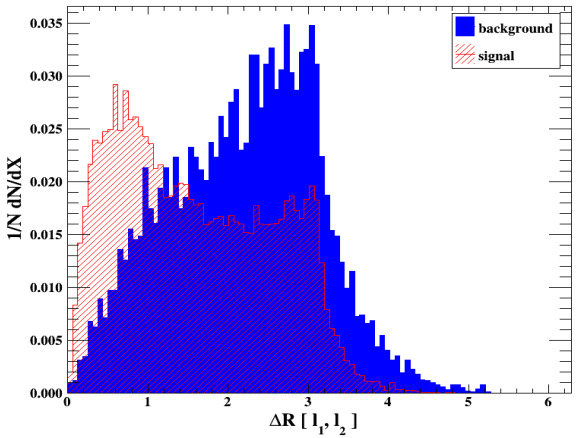

Figure: *The $\Delta R(\ell_1^{\pm}\ell_2^{\pm})$ distribution (normalized) between the two same-sign leptons for the positive scenario benchmark BP1.*

- (**C1-1**): Our signal event is hadronically quiet, hence, we put a veto on any jet with $p_T > 30$ GeV.
- (**C1-2**): Next, to confirm the trilepton signature, we select at least three leptons with $p_T > 10$ GeV.
- (**C1-3**): For further affirmation of trilepton signature, we reject any additional charged lepton with $p_T > 10$ GeV.
- (**C1-4**): Furthermore, we claim that the same flavor opposite sign (SFOS) lepton invariant mass $\mathrm{M}_{\ell^+\ell^-}$ should not lie between the window of 80-100 GeV to ensure that those are not directly produced from Z boson.

$3\ell^{\pm} + \not{E}_T$

- (**C1-5**): Finally, our signal events are required to have $\not{E}_T > 30$ GeV.
- (**C1-6**): The principal selection cut for the same-sign dilepton has been imposed. For this, we demand $\Delta R(\ell_1^{\pm}\ell_2^{\pm}) < 1.5$.

		Effective cross section (fb) for background after the cut						
SM-background	Production Cross section (fb)	C1–1	C1–2	C1–3	C1–4	C1–5	C1–6	
t+jets	2.22×10^5	157.50	0	0	0	0	0	
$t\bar{t}$+jets	7.07×10^5	420.37	0	0	0	0	0	
$W^{\pm}$+jets	1.54×10^8	4.96×10^7	0	0	0	0	0	
Z+jets	4.54×10^7	1.37×10^7	0	0	0	0	0	
W^+W^-+jets	8.22×10^4	4.76×10^3	0	0	0	0	0	
ZZ+jets	1.10×10^4	6.17×10^2	10.05	5.77	0.08	0.04	~ 0	
$W^{\pm}Z$+jets	3.81×10^4	1.71×10^3	42.40	42.40	0.72	0.36	0.04	
W^+W^-Z	83.10	1.17	0.09	0.07	0.01	~ 0	0	
$W^{\pm}ZZ$	26.80	0.39	0.03	0.03	~ 0	0	0	
$t\bar{t} + W^{\pm}$	360	0.13	0.02	~ 0	0	0	0	
$t\bar{t} + Z$	585	0.15	0.02	0.01	~ 0	0	0	
$t\bar{t} + h$	400	0.02	~ 0	0	0	0	0	
Total SM Background	2.005×10^8	6.33×10^7	52.60	48.30	0.81	0.40	0.04	
Positive scenario	Production Cross section (fb)	Effective cross section (fb) for signal after the cut						Luminosity (in fb^{-1}) for 5σ significance
BP1	185.10	0.75	0.20	0.14	0.08	0.06	0.040	1250.0
BP2	158.70	0.65	0.16	0.11	0.06	0.05	0.034	1600.4
Negative scenario	Production Cross section (fb)	Effective cross section (fb) for signal after the cut						Luminosity (in fb^{-1}) for 5σ significance
BP1	153.80	0.63	0.16	0.11	0.06	0.05	0.033	1675.8
BP2	134.70	0.55	0.15	0.10	0.05	0.04	0.030	1944.4

Table: *Effective cross section obtained after each cut for both signal ($3\ell^{\pm} + \not{E}_T$) and background and the respective required integrated luminosity for* 5σ significance at 13 TeV LHC.

$3\ell^{\pm} + \not{E}_T$

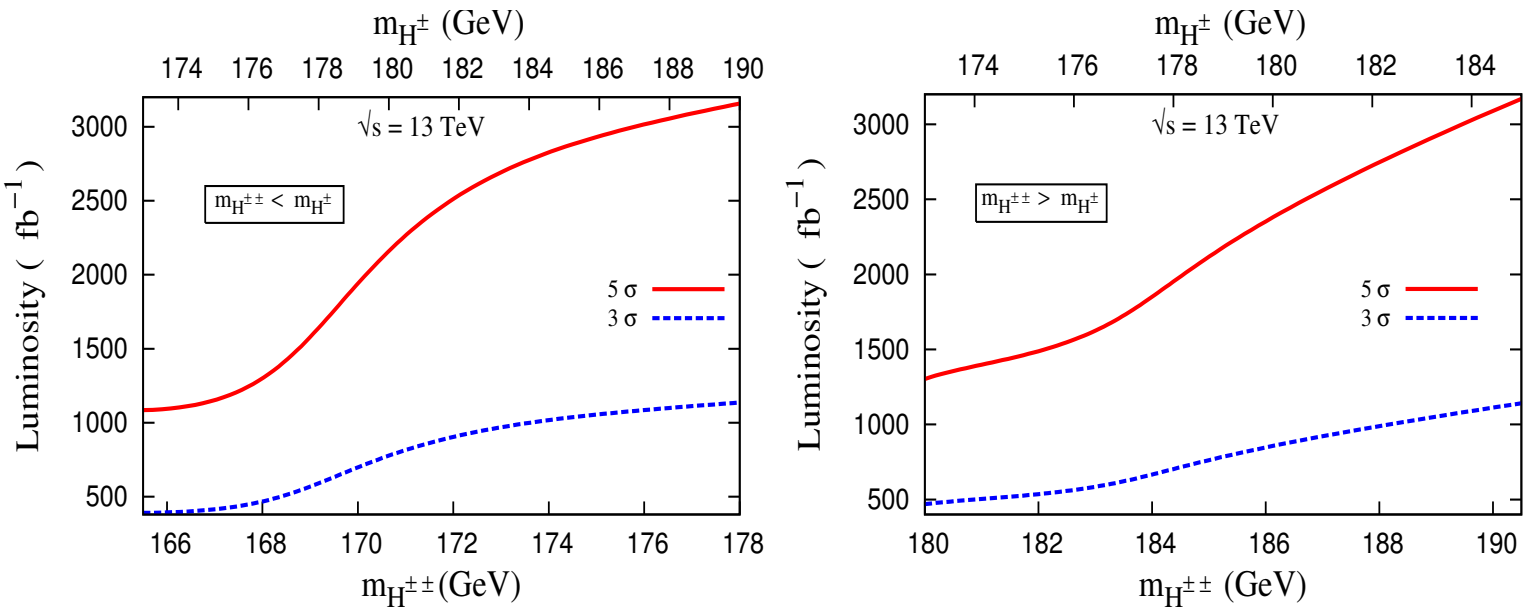

Figure: *Left (Right) panel shows the required integrated luminosity for* $3\ell^{\pm} + \not{E}_T$ *final state with respect to charged Higgs masses at the LHC at* $\sqrt{s} = 13$ TeV *for positive (negative) scenario. The solid red coloured and blue coloured dashed curve correspond to constant signal significance at* 5σ and 3σ respectively.

$2\ell^{\pm} + 4j + \not{E}_T$

$$\begin{aligned} pp \to H^{++}H^{--} &\to (W^+W^+) + (W^-W^-) \to (\ell^+\ell^+) + 4j + \not{E}_T \\ pp \to H^{++}H^{-} &\to (W^+W^+) + (W^-Z) \to (\ell^+\ell^+) + 4j + \not{E}_T \,. \end{aligned} \tag{15}$$

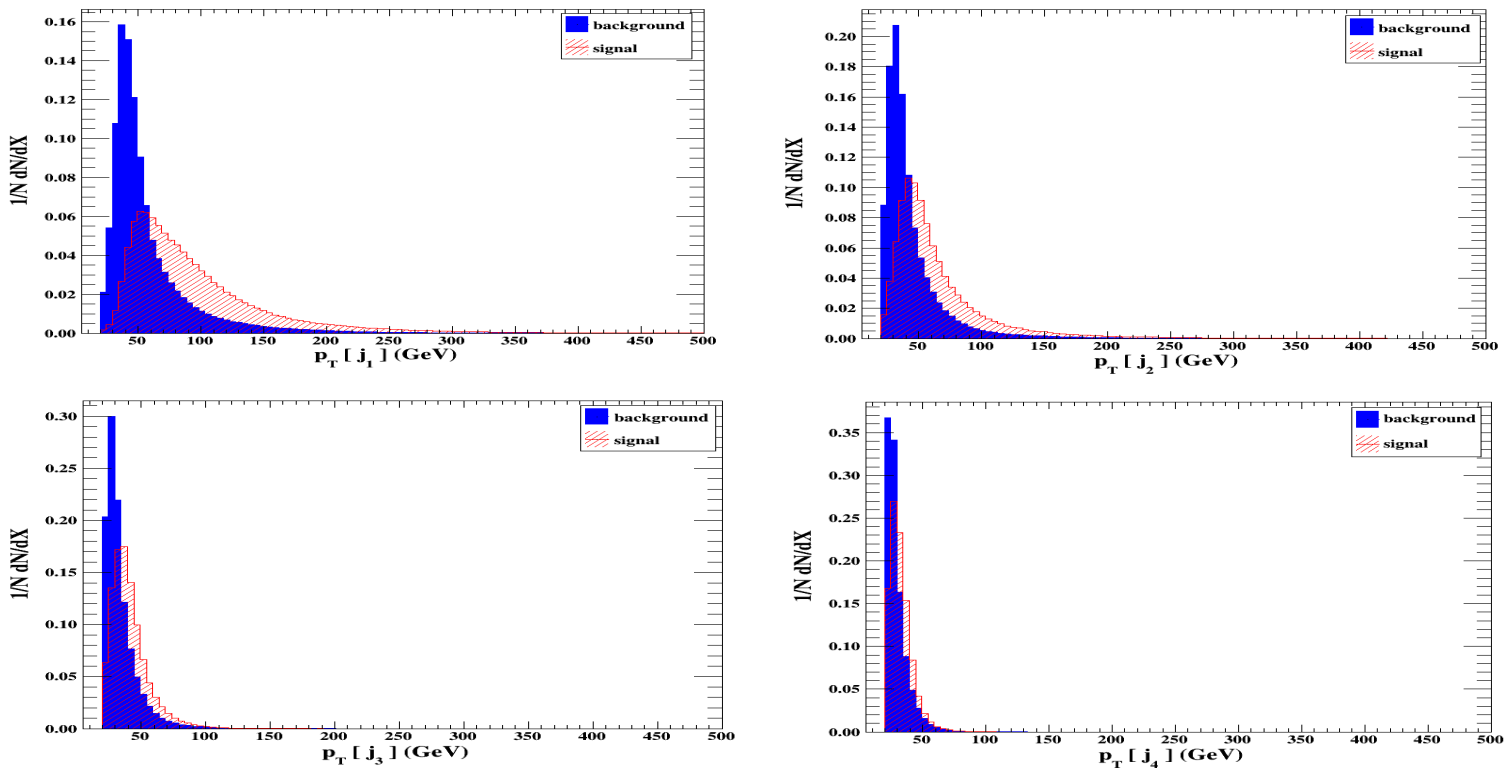

Figure: *Transverse momentum (p_T) distribution (normalized) of the four leading jets for the final state $2\ell^{\pm} + 4j + \not{E}_T$ for the benchmark BP1 of positive scenario.*

$2\ell^{\pm} + 4j + \not{E}_T$

- (**C2-1**): As explained, our signal is exempted from any b-jets, hence we can safely reject events with b-tagged jets of $p_T(b) > 40$ GeV.
- (**C2-2**): To guarantee that only 4 jets are present in the events, we reject any additional jets with $p_T(j_5) > 20$ GeV.
- (**C2-3**): Our signal also contains two isolated charged lepton and thus a veto on any additional leptons with $p_T > 10$ GeV is applied.
- (**C2-4**): Now, from the jet distribution, we choose the p_T of the leading jet to be at least greater than $p_T(j_1) > 60$ GeV.
- (**C2-5**): Moreover, for the next sub-leading jet we demand $p_T(j_2) > 40$ GeV to further subdue the background events.

$2\ell^{\pm} + 4j + \not{E}_T$

- (**C2-6**): A decent selection cut on the missing transverse energy is then applied as $\not{E}_T > 30$ GeV.
- (**C2-7**): Finally, the principal selection cut for the same-sign dilepton has been imposed. For this, we demand $\Delta R(\ell_1^{\pm}\ell_2^{\pm}) < 1.5$.

		Effective cross section (fb) after the cut							
SM-background	Production Cross section (fb)	C2–1	C2–2	C2–3	C2–4	C2–5	C2–6	C2–7	
t+jets	2.22×10^5	8.46×10^4	8.01×10^4	8.01×10^4	4.89×10^4	3.44×10^4	1.54×10^4	0	
$t\bar{t}$+jets	7.07×10^5	1.58×10^5	1.23×10^5	1.23×10^5	9.92×10^4	8.15×10^4	5.58×10^4	0	
$W^{\pm}$+jets	1.54×10^8	1.52×10^8	1.52×10^8	1.52×10^8	1.24×10^7	8.17×10^6	1.75×10^6	0	
Z+jets	4.54×10^7	4.27×10^7	4.27×10^7	4.27×10^7	3.76×10^6	2.48×10^6	4.65×10^5	0	
W^+W^-+jets	8.22×10^4	7.84×10^4	7.55×10^4	7.55×10^4	3.48×10^4	2.39×10^4	1.04×10^4	0	
ZZ+jets	1.10×10^4	8.96×10^3	8.67×10^3	8.65×10^3	4.27×10^3	2.89×10^3	1.16×10^3	0.05	
$W^{\pm}Z$+jets	3.81×10^4	3.33×10^4	3.13×10^4	3.12×10^4	1.67×10^4	1.18×10^4	5.76×10^3	1.68	
$t\bar{t} + W^{\pm}$	360	78.00	55.15	55.00	47.00	39.80	33.00	0.13	
$t\bar{t} + Z$	585	110.00	68.20	67.00	59.60	52.04	44.30	0.04	
$t\bar{t} + h$	400	46.00	27.40	27.20	24.50	21.65	18.30	0.04	
Total SM Background	2.005×10^8	1.95×10^8	1.94×10^8	1.94×10^8	1.64×10^7	1.08×10^7	2.31×10^6	1.94	
Positive scenario	Production Cross section (fb)	Effective cross section (fb) for signal after the cut							Luminosity (in fb^{-1}) for 5σ significance
BP1	311.40	253.00	210.70	206.70	181.72	158.90	126.24	1.90	26.6
BP2	259.30	211.23	175.92	172.64	151.75	132.66	105.42	1.55	36.3
Negative scenario	Production Cross section (fb)	Effective cross section (fb) for signal after the cut							Luminosity (in fb^{-1}) for 5σ significance
BP1	246.23	200.00	166.50	163.32	143.61	125.54	99.76	1.50	38.2
BP2	219.30	177.74	148.03	145.22	127.70	111.63	88.71	1.30	47.9

Table: *Effective cross section obtained after each cut for both signal ($2\ell^{\pm} + 4j + \not{E}_T$) and background and the respective required integrated luminosity for* 5σ significance at 13 TeV LHC.

$2\ell^{\pm} + 4j + \not{E}_T$

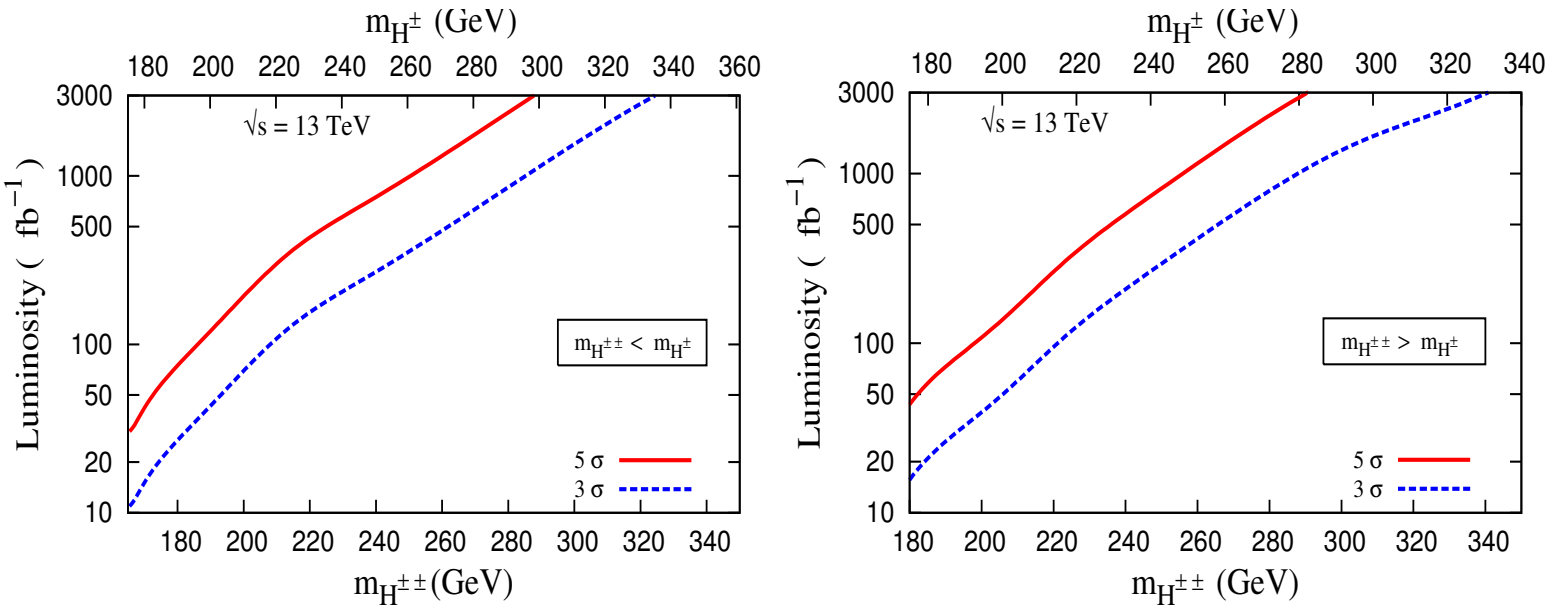

Figure: *Left (Right) panel shows the required integrated luminosity for* $2\ell^{\pm} + 4j + \not{E}_T$ *final state with respect to charged Higgs masses at the LHC at* $\sqrt{s} = 13$ TeV *for positive (negative) scenario.*

Conclusion

- We have found that the additional scalar fields can certainly surmount the instability problem and provide us with an absolutely stable vacuum even up to the Planck scale.
- We have chosen two distinct values of the triplet vev v_t (1 and 3 GeV) and have observed that the requirement of an absolutely stable vacuum up to the high Planck scale have pushed the neutral scalar mixing angle (α) to a quite small range of value for the non-degenerate mass scenario ($m_H(m_A) \gg m_h$) and peaks around a small positive value for considerably large m_H.
- Depending on the mass hierarchy, two possible scenarios (positive and negative) exist which however, at the end, yielded similar signal significance. In the allowed parameter space, with appreciable production cross section, the masses of the charged scalar can presumably be chosen around 200 GeV.
- Two specific final states at the collider, $(3\ell^{\pm} + \not{E}_T)$ and $(2\ell^{\pm} + 4j + \not{E}_T)$ at the 13 TeV LHC run. A proper cut-based analysis with detector simulation reveals that the first channel can only be probed at the 13 TeV LHC with high integrated luminosity around 1200 fb^{-1} and should be promoted for a HL-LHC. On the other hand, for the second channel we have found that even a 5σ discovery reach is possible with the present LHC data with only around 40 fb^{-1} luminosity.


Thank
you!!

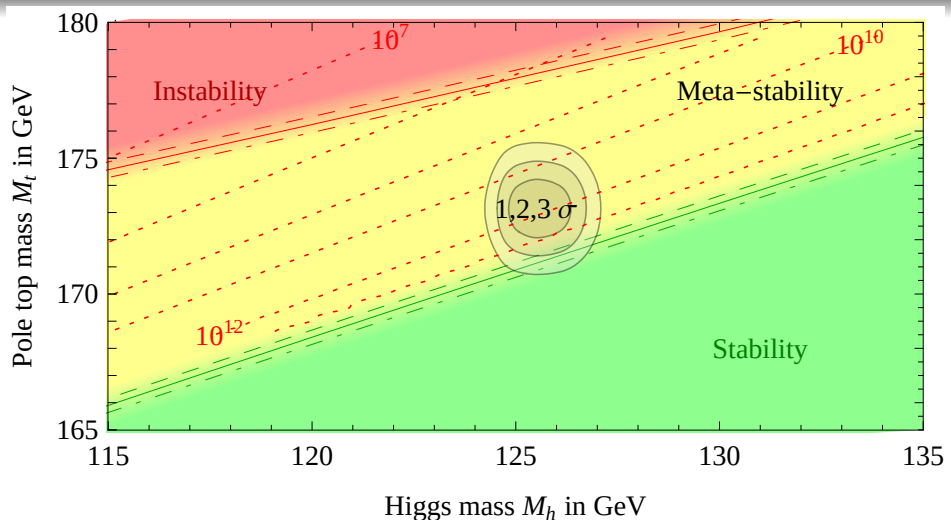

Here, we will present the one loop RGEs of all the relevant couplings (gauge, Yukawa and scalar quartic couplings) of the Type-II seesaw model[M. A. Schmidt et at, PhysRevD.76.073010]. For convenience, we introduce the shorthand notation $\mathcal{D} \equiv 16\pi^2 \frac{\mathrm{d}}{\mathrm{d}(\ln\mu)}$.

Gauge and top Yukawa couplings: The RGE for the gauge couplings,

$$\mathcal{D}g_1 = \frac{47}{10} {g_1}^3 , \tag{16a}$$

$$\mathcal{D}g_2 = -\frac{5}{2} g_2^3 , \tag{16b}$$

$$\mathcal{D}g_3 = -7 g_3^3 . \tag{16c}$$

The RGE for the top Yukawa coupling,

$$\mathcal{D}y_t = y_t\left(\frac{9}{2}y_t^2 - \left(8g_3^2 + \frac{9}{4}g_2^2 + \frac{17}{20}{g_1}^2\right)\right), \tag{16d}$$

where, $g_1 = \sqrt{\frac{5}{3}}g'$ with GUT renormalization.

Scalar quartic couplings: We express the RGEs of the scalar quartic coupling with a redefinition of the coupling to match with the potential notation of Ref. [**?**] which can be translated from our notation in the following way.

$$\Lambda_0 = \frac{\lambda}{2}, \tag{17a}$$
$$\Lambda_1 = 2\lambda_2 + 2\lambda_3, \tag{17b}$$
$$\Lambda_2 = -2\lambda_3, \tag{17c}$$
$$\Lambda_4 = \lambda_1 + \frac{\lambda_4}{2}, \tag{17d}$$
$$\Lambda_5 = -\frac{\lambda_4}{2}. \tag{17e}$$

The RGEs for the five quartic couplings that appear are then given by,

$$\mathcal{D}\Lambda_i = \beta_{\Lambda_i} + G_i\,, (i = 0, 1, 2, 4, 5)\,, \tag{18}$$

where, β_{Λ_i} and G_i are as follows:

$$\begin{aligned}
\beta_{\Lambda_0} &= 12\Lambda_0^2 + 6\Lambda_4^2 + 4\Lambda_5^2\,, && \text{(19a)}\\
\beta_{\Lambda_1} &= 14\Lambda_1^2 + 4\Lambda_1\Lambda_2 + 2\Lambda_2^2 + 4\Lambda_4^2 + 4\Lambda_5^2\,, && \text{(19b)}\\
\beta_{\Lambda_2} &= 3\Lambda_2^2 + 12\Lambda_1\Lambda_2 - 8\Lambda_5^2\,, && \text{(19c)}\\
\beta_{\Lambda_4} &= \Lambda_4\left(8\Lambda_1 + 2\Lambda_2 + 6\Lambda_0 + 4\Lambda_4 + 8\Lambda_5^2\right)\,, && \text{(19d)}\\
\beta_{\Lambda_5} &= \Lambda_5\left(2\Lambda_1 - 2\Lambda_2 + 2\Lambda_0 + 8\Lambda_4\right)\,, && \text{(19e)}
\end{aligned}$$

and,

$$\begin{aligned}
G_0 &= \left(12y_t^2 - \left(\frac{9}{5}g_1^2 + 9g_2^2\right)\right)\Lambda_0 + \frac{9}{4}\left(\frac{3}{25}g_1^4 + \frac{2}{5}g_1^2g_2^2 + g_2^4\right) - 12y_t^4\,, && \text{(20a)}\\
G_1 &= -\left(\frac{36}{5}g_1^2 + 24g_2^2\right)\Lambda_1 + \frac{108}{25}g_1^4 + 18g_2^4 + \frac{72}{5}g_1^2g_2^2\,, && \text{(20b)}\\
G_2 &= -\left(\frac{36}{5}g_1^2 + 24g_2^2\right)\Lambda_2 + 12g_2^4 - \frac{144}{5}g_1^2g_2^2\,, && \text{(20c)}\\
G_4 &= \left(6y_t^2 - \left(\frac{9}{2}g_1^2 + \frac{33}{2}g_2^2\right)\right)\Lambda_4 + \frac{27}{25}g_1^4 + 6g_2^4\,, && \text{(20d)}\\
G_5 &= \left(6y_t^2 - \left(\frac{9}{2}g_1^2 + \frac{33}{2}g_2^2\right)\right)\Lambda_5 - \frac{18}{5}g_1^2g_2^2\,. && \text{(20e)}
\end{aligned}$$

Basic cuts

In our signal and background events, we select jets and leptons using the following basic kinematical acceptance cuts :

$$\Delta R_{jj} > 0.6, \quad \Delta R_{\ell\ell} > 0.4, \quad \Delta R_{j\ell} > 0.7\,, \tag{21a}$$

$$\Delta R_{bj} > 0.7, \quad \Delta R_{b\ell} > 0.2, \tag{21b}$$

$$p^{j}_{T_{\min}} > 20\ \mathrm{GeV}, \quad |\eta_j| < 5, \tag{21c}$$

$$p^{\ell}_{T_{\min}} > 10\ \mathrm{GeV}, \quad |\eta_\ell| < 2.5, \tag{21d}$$

b-jet abiding by the efficiency as proposed by the ATLAS collaboration [**?**]:

$$\epsilon_b = \begin{cases} 0 & p^b_T \leq 30\ \mathrm{GeV} \\ 0.6 & 30\ \mathrm{GeV} < p^b_T < 50\ \mathrm{GeV} \\ 0.75 & 50\ \mathrm{GeV} < p^b_T < 400\ \mathrm{GeV} \\ 0.5 & p^b_T > 400\ \mathrm{GeV}\ . \end{cases} \tag{22}$$